



Arabidopsis receptor-like cytoplasmic kinase BIK1: purification, crystallization and X-ray diffraction analysis

Neeraj K. Lal,^a Andrew J. Fisher^{b*} and Savithamma P. Dinesh-Kumar^{a*}

Received 4 July 2016

Accepted 23 August 2016

Keywords: receptor-like kinase; receptor-like cytoplasmic kinases; RLCK; BIK1; BOTRYTIS-INDUCED KINASE 1; PAMP-triggered immunity; *Arabidopsis*.

Supporting information: this article has supporting information at journals.iucr.org/f

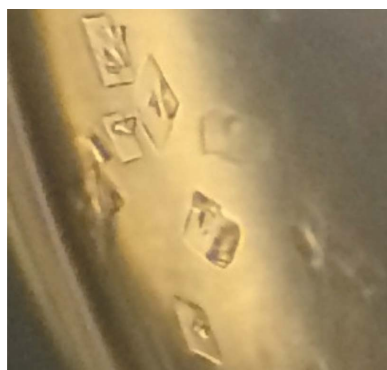
^aDepartment of Plant Biology and The Genome Centre, College of Biological Sciences, University of California, Davis, CA 95616, USA, and ^bDepartment of Chemistry and Department of Molecular, Cellular and Developmental Biology, University of California, Davis, CA 95616, USA. *Correspondence e-mail: ajfisher@ucdavis.edu, spdineshkumar@ucdavis.edu

Receptor-like cytoplasmic kinases (RLCKs) in *Arabidopsis* play a central role in the integration of signaling input from various growth and immune signaling pathways. BOTRYTIS-INDUCED KINASE 1 (BIK1), belonging to the RLCK family, is an important player in defense against bacterial and fungal pathogens and in ethylene and brassinosteroid hormone signaling. In this study, the purification and crystallization of a first member of the class VI family of RLCK proteins, BIK1, are reported. BIK1 was crystallized using the microbatch-under-oil method. X-ray diffraction data were collected to 2.35 Å resolution. The crystals belonged to the monoclinic space group *C*2, with two monomers per asymmetric unit.

1. Introduction

Receptor-like cytoplasmic kinase (RLCK) proteins belong to a larger receptor-like kinase (RLK) superfamily with more than 600 members in *Arabidopsis* (Shiu & Bleecker, 2003; Antolín-Llovera *et al.*, 2012). The RLK superfamily constitutes 2.5% of protein-coding genes in *Arabidopsis* and typically contains proteins with both serine threonine and tyrosine kinase activity (Shiu & Bleecker, 2001; Macho *et al.*, 2015). Members of the RLCK subfamily of the RLK superfamily lack a receptor ectodomain and transmembrane region; however, they still localize to the plasma membrane either through post-translational modifications such as acylation or through their association with membrane-bound RLKs to relay information from the cell surface to the cytosol (Veronese *et al.*, 2006; Tang *et al.*, 2008). RLCK members are similar to mammalian kinases, with a small N-terminal lobe and a large C-terminal lobe (Antolín-Llovera *et al.*, 2012). In addition to the conserved kinase core, some plant RLCKs also contains N- and C-terminal extensions with unknown function. The function of most RLCK members remains unknown, but recent findings have suggested that RLCK members play an essential role in various physiological processes such as growth, differentiation, disease resistance and hormone responses (Tang *et al.*, 2008; Kim *et al.*, 2011; Laluk *et al.*, 2011; Liu *et al.*, 2011; Lu *et al.*, 2010; Burr *et al.*, 2011; Bayer *et al.*, 2009).

One of the well studied members of the RLCK subfamily is BOTRYTIS INDUCED KINASE 1 (BIK1), which is a shared component of both growth and immune signaling pathways (Lin *et al.*, 2013). BIK1 was initially identified based on its role in ethylene hormone-mediated defense signaling and its role in defense against the fungal pathogens *Botrytis cinerea* and *Alternaria brassicicola* (Veronese *et al.*, 2006). BIK1 acts as a



negative regulator of BRASSINOSTEROID INSENSITIVE 1 (BRI1) growth-hormone signaling (Lin *et al.*, 2013). BRI1 recognizes brassinosteroids through its extracellular leucine-rich repeat (LRR) domain to initiate downstream signal transduction with phosphorylation and dissociation of BIK1 from BRI1 (Lin *et al.*, 2013). Similarly, during immune signaling bacterial flagellin is recognized by the extracellular LRR domain of FLAGELLIN SENSING 2 (FLS2), which leads to BIK1 phosphorylation and disassociation from FLS2 (Lu *et al.*, 2010; Zhang *et al.*, 2010). In addition, BIK1 associates with PEP RECEPTOR 1 (PEPR1) and PEPR2 RLKs that recognize endogenous danger-associated molecular patterns (DAMPs) to trigger immune responses (Liu *et al.*, 2013). A recent study suggested that BIK1 interacts with and phosphorylates RbohD to modulate reactive oxygen species (ROS) burst during innate immunity (Kadota *et al.*, 2014; Li *et al.*, 2014). Therefore, accumulating evidence indicates that BIK1 functions as a positive regulator of immunity (Laluk *et al.*, 2011; Lu *et al.*, 2010, Lin *et al.*, 2013; Liu *et al.*, 2013) and as a negative regulator of growth signaling (Laluk *et al.*, 2011; Lin *et al.*, 2013).

The kinase activity of BIK1 is important for BIK1-mediated signaling (Lin *et al.*, 2014). However, the precise mechanism by which BIK1 phosphorylation leads to its activation and downstream signaling remains unknown. Here, we report preliminary crystallization data for BIK1 in order to further study the molecular mechanisms by which phosphorylation of BIK1 leads to its differential role in growth and immune signaling.

2. Materials and methods

2.1. Macromolecule production

The coding region of BIK1 (AT2G39660) was amplified from a homemade *Arabidopsis* Col-0 ecotype cDNA library using primer 1 (CACCATGAAAACCTGTACTTCCAATC-CAATATGGGTTCTTGC TTCAGTTCTCGAGTCAA) and primer 2 (GCGATCGCGGATCCGTTATCCACTTCCAA-TCTACACAAGGTGCCTGCCAAAAGGTTTTT). To clone BIK1 into Macro Lab His-TEV expression vector (Addgene No. 29666), the vector was linearized using the SspI restriction enzyme for 3 h at 310 K. The purified PCR product was cloned into linearized vector using Gibson assembly and the resulting product was transformed into DH10B *Escherichia coli* cells (Gibson *et al.*, 2009). The resulting plasmid clones were sequenced using T7 promoter (TAATACGACTCACTATA-GGG) and T7 terminator (GCTAGTTATTGCTCAGCGG) primers. Sequence-confirmed BIK1 plasmid was transformed into *E. coli* strain BL21 and cultured overnight at 310 K in LB medium containing 100 µg ml⁻¹ ampicillin. 5 ml of overnight-grown culture was used to inoculate 1 l 2 × YT liquid medium (RPI Corporation) for large-scale growth. Once the OD₆₀₀ of culture had reached 0.6, the cells were cooled on ice and induced with 100 µM isopropyl β-D-1-thiogalactopyranoside (IPTG) at 291 K for 16 h. The next day, the cells were harvested by centrifugation at 6037g for 15 min. The super-

natant was discarded and the pelleted cells were resuspended in buffer A (30 mM HEPES, 200 mM NaCl, 20 mM imidazole, 2 mM β-mercaptoethanol pH 7.5) and lysed using a microfluidizer. The lysate was centrifuged at 40 000g to separate insoluble cell debris, and the supernatant was incubated with HisPure cobalt resin (Thermo Fisher Scientific) for 1 h at 277 K with constant shaking. The resin was washed with five column volumes of buffer A and eluted in buffer A plus 500 mM imidazole. The eluate from the cobalt resin was diluted with three volumes of buffer A and loaded onto a HiTrap SP 5 ml column (GE Healthcare). The bound protein was eluted with a gradient of 0.1–1 M NaCl in 30 mM HEPES pH 7.5 buffer. The peak fractions from ion exchange were concentrated and loaded onto a HiLoad 16/600 Superdex prep-grade size-exclusion column at 277 K. Fractions containing BIK1 were collected and incubated with TEV protease with an N-terminal His tag in a 1:2 molar ratio for 16 h at 277 K. The next day, the TEV protease and cleaved His tag from BIK1 were removed by incubation with cobalt resin. The flowthrough from the cobalt column containing BIK1 was concentrated and loaded onto a HiLoad 16/600 Superdex PG size-exclusion column equilibrated with 10 mM HEPES, 150 mM NaCl, 2 mM β-mercaptoethanol pH 7.2. The peak fractions were concentrated, flash-frozen in liquid nitrogen at 5 mg ml⁻¹ and stored at 193 K. The purity of the protein was estimated to be greater than 90% on an SDS-PAGE gel. The yield of BIK1 was 0.5 mg per litre of culture. Purified BIK1 was incubated with or without 0.1 mM ATP, 5 mM MgCl₂ and immunoblotting was performed with anti-phosphotyrosine antibody (α-pY; Cell Signaling) to conform the kinase activity

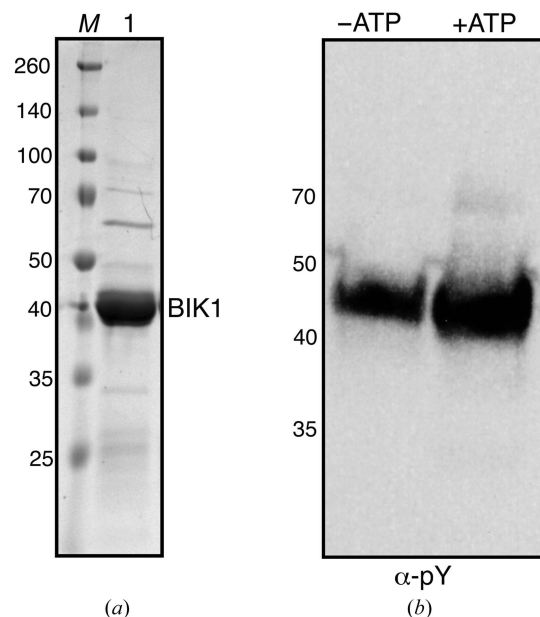


Figure 1 BIK1 purified from *E. coli* is an active kinase. (a) SDS-PAGE analysis of purified BIK1 from *E. coli*. Coomassie-stained gel showing BIK1 protein after size-exclusion chromatography (lane 1) and a broad-range protein ladder (lane M). The sizes of the protein ladder are indicated on the left in kDa. (b) The purified BIK1 protein (–ATP) or BIK1 protein incubated with 0.1 M ATP and 5 mM MgCl₂ were separated on SDS-PAGE and immunoblotted with anti-phosphotyrosine antibody (α-pY).

Table 1
Macromolecule-production information.

Source organism	<i>Arabidopsis</i>
DNA source	<i>Arabidopsis</i> Col-0 cDNA
Forward primer	CACCATGAAAACCTGTACTTCCAATCCAATATGGGTTCTTGCTTCAGTTCTCGAGTCAA
Reverse primer	GCGATCGCGGATCCGTTATCCCACTTCCAATCTACACAA-GGTGCCTGCCAAAAGGTTTT
Cloning vector	pET His6 TEV LIC (Addgene No. 29666)
Expression vector	Same as the cloning vector
Expression host	<i>E. coli</i> BL21 (DE3)
Complete amino-acid sequence of the construct produced†	<u>MKSSHHHHHENLYFQSNMGSCFSSRVKADIFHNGKSS-DLYGLSLSSRKSSSTVAAAQKTEGEILSSSTPVKSF</u> FNLKLA TRNFRPDSVIGEGGFCVFKGWLDESTLT- PTKPGTGLVIAVKKLNQEGFQGHREWLTEINYLGL- SHPNLVKLIGYCLEDEHRLLVYEFMQKGSLENHLFR- RGAYFKPLPWFLRVNVALDAKGLAFLHSDPVKVIY- RDIKASNILLDADYNKLSDFGLARDGPMGDLSYVS- TRVMGTGYAAPEYMSSGHLNARSDVYSFGVLLLEI- LSGKRALDHNRPAKEENLVDWARPYLTSKRKVLITV- DNRLDTQYLPEEAVRMAVAVQCLSFEPKSRPTMDQ- VVRALQQLQDNLGKPSQTNPKVDTKKGFKTGTTKS- SEKRFTQKPFGRHLV

† The additional N-terminal residues of the hexahistidine tag followed by the TEV cleavage site are underlined in the amino-acid sequence of the construct produced.

of the purified protein (Fig. 1). Interestingly, BIK1 is a hyperactive kinase (Lin *et al.*, 2013) and is phosphorylated during expression and purification. There was no major change in the phosphorylation status of BIK1 upon incubation with ATP (Fig. 1). A summary of macromolecule production is given in Table 1.

2.2. Crystallization

Crystallization was performed by the batch method under paraffin oil at 291 K. Initial crystallization conditions were screened using 1536 conditions: 848 from commercial crystallization screens (Crystal Screen HT, Index, PEGRx HT, SaltRx HT, PEG/Ion HT, Slice pH, Ionic Liquid, Polymer Screen and Silver Bullets from Hampton Research) and 688



Figure 2
Crystals of *Arabidopsis* BIK1 grown in 245 mM ammonium tartrate, 12.5% PEG 3350 pH 7.0.

Table 2
Crystallization.

Method	Microbatch under oil
Plate type	72-well
Temperature (K)	293
Protein concentration (mg ml ⁻¹)	3.3
Buffer composition of protein solution	10 mM HEPES, 150 mM NaCl, 2 mM β-mercaptoethanol pH 7.2
Composition of reservoir solution	245 mM ammonium tartrate, 12.5% PEG 3350 pH 7.0
Volume and ratio of drop	2 μl final volume, 1:1 ratio of protein:reservoir

Table 3
Data collection and processing.

Diffraction source	Beamline 12-2, SSRL
Wavelength (Å)	0.9795
Temperature (K)	100
Detector	PILATUS 6M
Crystal-to-detector distance (mm)	400
Rotation range per image (°)	0.2
Total rotation range (°)	150
Exposure time per image (s)	0.2
Beam attenuation (%)	50
Beam size (μm)	50
Space group	C2
Unit-cell parameters (Å, °)	$a = 114.2, b = 72.1, c = 93.9,$ $\alpha = 90, \beta = 108.41, \gamma = 90$
Mosaicity (°)	0.11–0.24
Resolution range (Å)	50.0–2.35 (2.41–2.35)
Total No. of reflections	85875 (6217)
No. of unique reflections	29382 (2146)
Completeness (%)	96.6 (95.1)
Multiplicity	2.92 (2.90)
$\langle I/\sigma(I) \rangle$	9.73 (1.93†)
R_{meas} (%)	8.1 (57.5)
Overall B factor from Wilson plot (Å ²)	26.8

† Although $I/\sigma(I)$ is less than 2.0 in the highest resolution shell, $CC_{1/2}$ is 88.3 in this shell.

from homemade screens with various PEG/salt/buffer. Initial screening produced microcrystals in PEG 3350 and ammonium salts. Crystallization with PEG 3350 was optimized by changing variables such as the pH and buffers and using various ammonium salts. About 4–5 d after setup, small crystals appeared in ammonium tartrate and PEG 3350. These conditions were further optimized by varying the concentrations of protein and of salt and the PEG concentration, along with the ratio of paraffin and silicone oil to control the rate of diffusion (D'Arcy *et al.*, 2003). Ultimately, crystals of maximum dimensions 0.2 × 0.2 mm grew after 4–5 d in 245 mM ammonium tartrate, 12.5% PEG 3350 pH 7, with a final protein concentration of 3.3 mg ml⁻¹, using a 1:1 ratio of paraffin to silicon oil. The crystallization details are summarized in Table 2.

2.3. Data collection and processing

Crystals were transferred to reservoir solution supplemented with 25% ethylene glycol as a cryoprotectant. After soaking for ~5 s, the crystals were mounted on a cryoloop and flash-cooled in liquid nitrogen. X-ray diffraction data for BIK1 were collected on beamline 12-2 at Stanford Synchrotron Radiation Lightsource (SSRL). Diffraction intensity data

were processed using *XDS* (Kabsch, 2010a) and scaled with *XSCALE* (Kabsch, 2010b). Table 3 shows a summary of data collection.

3. Results and discussion

Recombinant *Arabidopsis* BIK1 was expressed and purified from *E. coli* BL21 (DE3) cells using a three-step purification strategy (affinity, ion-exchange and size-exclusion chromatography). The purified BIK1 is an active kinase demonstrating autophosphorylation activity (Fig. 1). Initial small microcrystals ($\sim 5\ \mu\text{m}$) were observed under several conditions with PEG 3350 and salt in batch screening. After various rounds of optimization, diffraction-quality crystals of $200\ \mu\text{m}$ in size were obtained in 245 mM ammonium tartrate, 12.5% PEG 3350 pH 7 (Fig. 2). The best crystals diffracted to a final resolution of 2.35 Å on beamline 12-2 at SSRL (Fig. 3) and belonged to the monoclinic space group *C2* (Table 1). There are predicted to be two BIK1 monomers in the crystallographic asymmetric unit based on a Matthews coefficient of $2.08\ \text{\AA}^3\ \text{Da}^{-1}$, resulting in a solvent content of $\sim 41\%$ (Matthews, 1968). A self-rotation function calculated using the diffraction data revealed a significant peak with a κ value of 180° that was 90% the height of the crystallographic twofold axis (Fig. 4). This indicates that a noncrystallographic twofold axis is situated approximately 18° from the unit-cell *a* axis perpendicular to the *b* axis (Fig. 4).

BIK1 belongs to the RLCK superfamily. RLCK family members share sequence similarity with the interleukin-1 receptor-associated kinase (IRAK)/Pelle protein kinase family (Shiu & Blecker, 2001, 2003). BIK1 is 37% identical to

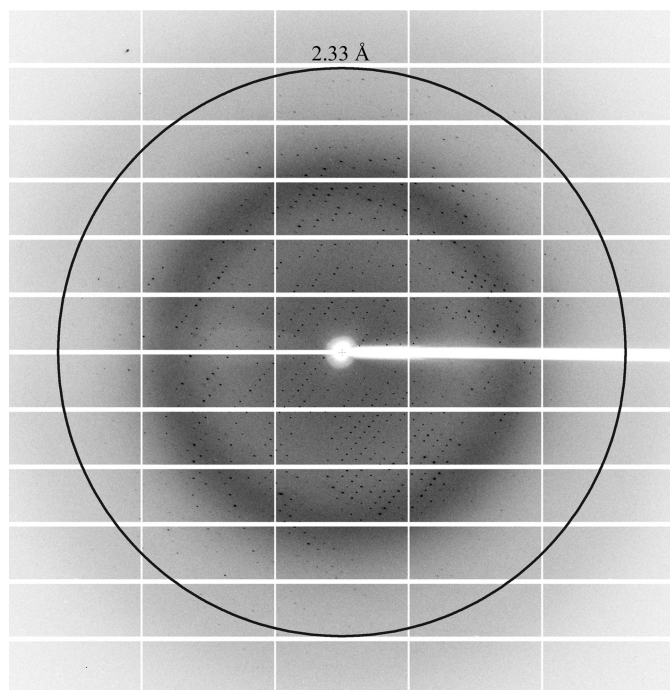


Figure 3
A typical diffraction pattern of a crystal of BIK1 obtained on SSRL beamline 12-2.

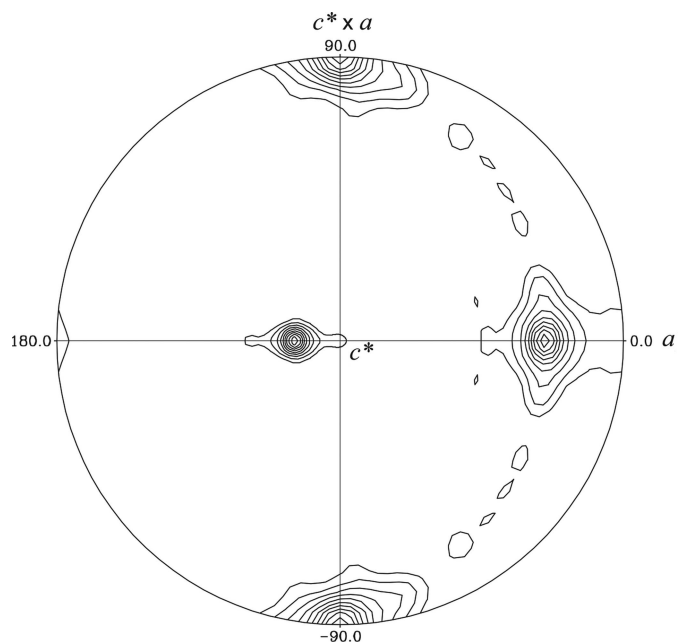


Figure 4
Self-rotation function of BIK1 X-ray diffraction data. The stereographic projection from *POLARRFN* in the *CCP4* suite (Winn *et al.*, 2011) corresponding to a rotation angle of $\kappa = 180^\circ$ is shown. The monoclinic crystallographic twofold *b* axis is vertical ($c^* \times a$ on the plot). A strong noncrystallographic twofold axis is also observed rotated $\sim 18^\circ$ from the monoclinic *a* axis (horizontal) perpendicular to the *b* axis. The rotation function was calculated using all data to a resolution of 2.35 Å and a radius of integration of 20 Å. The rotation-function map was contoured starting at the level of two root-mean-square (r.m.s.) deviations, with a contour interval at every one r.m.s. deviation of the calculated map.

IRAK4. In addition, BIK1 shares 36% identity with the cytoplasmic domain of BAK1 (BRI1-associated kinase 1) and 39% identity with the BAK1 kinase-domain sequence that has been crystallized (PDB entry 3uim; Yan *et al.*, 2012). We are currently solving the crystal structure of BIK1 by molecular replacement using BAK1 (PDB entry 3uim) and IRAK4 (PDB entry 2oib; Kuglstatter *et al.*, 2007) as search models. Additionally, we are currently pursuing co-crystallization of BIK1 with ATP analogues.

Acknowledgements

We thank UC Davis Research Investments in Science and Engineering (RISE) funds for supporting this work.

References

- Antolín-Llovera, M., Ried, M. K., Binder, A. & Parniske, M. (2012). *Annu. Rev. Phytopathol.* **50**, 451–473.
- Bayer, M., Nawy, T., Giglione, C., Galli, M., Meinel, T. & Lukowitz, W. (2009). *Science*, **323**, 1485–1488.
- Burr, C. A., Leslie, M. E., Orłowski, S. K., Chen, I., Wright, C. E., Daniels, M. J. & Liljegren, S. J. (2011). *Plant Physiol.* **156**, 1837–1850.
- D’Arcy, A., Mac Sweeney, A., Stihle, M. & Haber, A. (2003). *Acta Cryst.* **D59**, 396–399.
- Gibson, D. G., Young, L., Chuang, R.-Y., Venter, J. C., Hutchison, C. A. III & Smith, H. O. (2009). *Nature Methods*, **6**, 343–345.
- Kabsch, W. (2010a). *Acta Cryst.* **D66**, 125–132.
- Kabsch, W. (2010b). *Acta Cryst.* **D66**, 133–144.

- Kadota, Y., Sklenar, J., Derbyshire, P., Stransfeld, L., Asai, S., Ntoukakis, V., Jones, J. D., Shirasu, K., Menke, F., Jones, A. & Zipfel, C. (2014). *Mol. Cell*, **54**, 43–55.
- Kim, T.-W., Guan, S., Burlingame, A. L. & Wang, Z.-Y. (2011). *Mol. Cell*, **43**, 561–571.
- Kuglstatler, A., Villaseñor, A. G., Shaw, D., Lee, S. W., Tsing, S., Niu, L., Song, K. W., Barnett, J. W. & Browner, M. F. (2007). *J. Immunol.* **178**, 2641–2645.
- Laluk, K., Luo, H., Chai, M., Dhawan, R., Lai, Z. & Mengiste, T. (2011). *Plant Cell*, **23**, 2831–2849.
- Li, L., Li, M., Yu, L., Zhou, Z., Liang, X., Liu, Z., Cai, G., Gao, L., Zhang, X., Wang, Y., Chen, S. & Zhou, J.-M. (2014). *Cell Host Microbe*, **15**, 329–338.
- Lin, W., Li, B., Lu, D., Chen, S., Zhu, N., He, P. & Shan, L. (2014). *Proc. Natl Acad. Sci. USA*, **111**, 3632–3637.
- Lin, W., Lu, D., Gao, X., Jiang, S., Ma, X., Wang, Z., Mengiste, T., He, P. & Shan, L. (2013). *Proc. Natl Acad. Sci. USA*, **110**, 12114–12119.
- Liu, J., Elmore, J. M., Lin, Z.-J. & Coaker, G. (2011). *Cell Host Microbe*, **9**, 137–146.
- Liu, Z., Wu, Y., Yang, F., Zhang, Y., Chen, S., Xie, Q., Tian, X. & Zhou, J.-M. (2013). *Proc. Natl Acad. Sci. USA*, **110**, 6205–6210.
- Lu, D., Wu, S., Gao, X., Zhang, Y., Shan, L. & He, P. (2010). *Proc. Natl Acad. Sci. USA*, **107**, 496–501.
- Macho, A. P., Lozano-Durán, R. & Zipfel, C. (2015). *Trends Plant Sci.* **20**, 269–272.
- Matthews, B. W. (1968). *J. Mol. Biol.* **33**, 491–497.
- Shiu, S. H. & Bleecker, A. B. (2001). *Proc. Natl Acad. Sci. USA*, **98**, 10763–10768.
- Shiu, S. H. & Bleecker, A. B. (2003). *Plant Physiol.* **132**, 530–543.
- Tang, W., Kim, T.-W., Osés-Prieto, J. A., Sun, Y., Deng, Z., Zhu, S., Wang, R., Burlingame, A. L. & Wang, Z.-Y. (2008). *Science*, **321**, 557–560.
- Veronese, P., Nakagami, H., Bluhm, B., Abuqamar, S., Chen, X., Salmeron, J., Dietrich, R. A., Hirt, H. & Mengiste, T. (2006). *Plant Cell*, **18**, 257–273.
- Winn, M. D. *et al.* (2011). *Acta Cryst.* **D66**, 235–242.
- Yan, L., Ma, Y., Liu, D., Wei, X., Sun, Y., Chen, X., Zhao, H., Zhou, J., Wang, Z., Shui, W. & Lou, Z. (2012). *Cell Res.* **22**, 1304–1308.
- Zhang, J., Li, W., Xiang, T., Liu, Z., Laluk, K., Ding, X., Zou, Y., Gao, M., Zhang, X., Chen, S., Mengiste, T., Zhang, Y. & Zhou, J.-M. (2010). *Cell Host Microbe*, **7**, 290–301.